ACADEMIA ROMÂNĂ
Revue Roumaine de Chimie
https://www.icf.ro/rrch/

Rev. Roum. Chim.,
2025, *70*(7–8), 411–420
DOI: 10.33224/rrch.2025.70.7-8.05

Dedicated to the memory of
Academician Bogdan C. Simionescu (1948–2024)

EFFECTS OF DONOR-ACCEPTOR INTERACTIONS ON STRUCTURAL RELAXATION AND ELECTRICAL CONDUCTION OF POLYMERS OBSERVED BY DIELECTRIC SPECTROSCOPY

Cristian Vasile GRIGORAS,* Valentina Elena MUSTEATA,
Anca Giorgiana GRIGORAS and Virgil BARBOIU*

"Petru Poni" Institute of Macromolecular Chemistry, Aleea Grigore Ghica Voda 41A, Iasi-700487, Roumania

Received February 20, 2025

Dielectric permittivity spectra of a series of random methacrylate copolymers containing phenothiazinyl and 3,5-dinitrobenzoyl side groups of variable ratios were recorded at various temperatures over the glass transition range to investigate the effects of the donor-acceptor interactions density on the α-relaxation processes and electrical conduction. The process parameters were obtained by using the Havriliak-Negami equations. The dependence of relaxation on temperature was analyzed using the VFTH equation whose parameters were determined for each copolymer, *i.e.*, depending on the donor/acceptor ratio. As expected, the dependence of the Vogel-Fulcher temperature, relaxation time, dielectric glass transition temperature, and fragility deviates from monotony, showing maxima in the equimolar concentration region, where the probability of donor-acceptor interactions is also maximum.. Very interestingly, the electrical conduction was founded as a combination of two components, ionic and electronic, the second being clearly favored by donor-acceptor interactions.

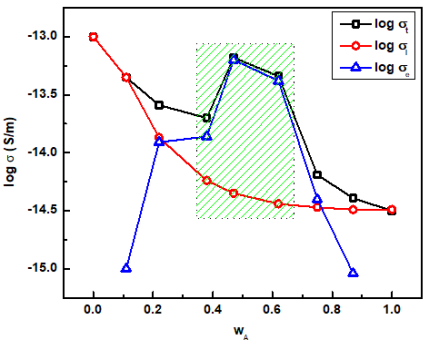

INTRODUCTION

Polymer systems containing both electron donor (ED) and electron acceptor (EA) components have diverse applications in which the effects induced by physical and chemical factors are used. Among these, illumination, electric field, temperature and environmental reactivity depend on donor-acceptor (D-A) interactions, in fact on the charge transfer process.[1] One of the first practical applications was in xerographic devices where the photosensitive element is a polymer layer comprising a small molecular compound containing ED groups and the EA groups respectively, for example, poly(N-vinyl carbazole) with trinitrofluorenone being a classical pair.[2] Photorefractive materials are also of interest.[3] More recently, donor-acceptor systems have received tremendous attention due to their application in emerging technologies such as organic solar cells.[4–6]

While the mixing approach has the advantage of the wide availability of a library of compounds with

* Corresponding author: crgrig@icmpp.ro

suitable band gaps for efficient charge transfer, it is expected that incorporating the donor and acceptor as pendant groups on the same macromolecular chain will overcome some disadvantages, such as phase separation due to chemical incompatibility and long-term device stability. Here, we investigated polymers containing different proportions of ED and EA groups, also known as donor-acceptor (D-A) copolymers, and showed the influence of the interactions between these groups on the solid-state properties, as inferred from the dielectric spectra, especially conductivity and α-relaxation. Early studies by Simionescu *et al.*[7–9] focused on the synthesis and D-A interactions in solution. These interactions were later revealed in the solid state by DSC[10,11] and photoconductivity measurements.[12–14]

The present study concerns the α-dielectric relaxation of polymers with phenothiazinyl and 3,5-dinitrobenzoyl groups as ED and EA side groups, respectively (Scheme 1). The literature reports that only a few studies related to dielectric relaxation spectroscopy (DRS) have been performed on copolymers with nonpolar and polar groups in different ratios.[15,16] To date, no similar work has been reported on D-A polymers or blends with ED and EA components, despite some interesting observations that have been obtained. Thus, it is likely that D-A interactions exert hindering effects on molecular dynamics similar to those of crosslinks,[17] which explains the positive deviations of the glass transition temperature (Tg) from the weighted average of the corresponding homopolymers.[18] Therefore, it can be assumed that the density and strength of D-A interactions have a strong influence on DRS parameters such as Vogel-Fulcher temperature, relaxation rate, brittleness, electrical conductivity and others. Furthermore, since the density of D-A interactions depends on the copolymer composition, which is further expressed by w_A, the molar fraction of acceptor units, it is expected that these parameters are composition-dependent. In terms of strength, these D-A interactions are weak, being of the π-π type between the aromatic rings of the D units, which are electron donors due to the amine substitution, and the aromatic rings of the A units, which are electron acceptors due to the nitro substitution. On the other hand, the interacting groups are spaced from the methacrylic backbone by flexible spacers long enough to move freely in the absence of D-A interactions (Scheme 1).

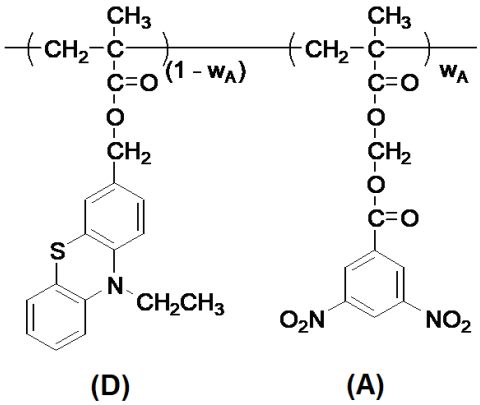

Scheme 1 – Chemical structure of the studied polymers.

The DRS measurements were done for each polymer composition in a wide range of frequencies and temperatures, covering the glass transition range. The dielectric α-relaxation time (τ) and d.c. electrical conductivity (σ) was obtained in the Havriliak-Negami (HN) approach.

The dependence between relaxation time and temperature (T) was processed by the well-known VFTH (Vogel-Fulcher-Tammann-Hesse) (eq. 1),[19–21] which, as is known, performs best when the deviation from Arrhenius behavior is neglected, particularly for $T > T_g + 50$ K.[22] Parameters in this equation are the T_v (Vogel-Fulcher temperature), considered as the configurationally ground-state temperature, *i.e.*, a hypothetical kinetic temperature associated with zero cooperative mobility, and τ_0, the relaxation time when $T \rightarrow \infty$, as well as some derived ones, were found and discussed function of polymer composition. The DRS glass transition temperature, T_{gDRS}, corresponding to the state of whose α-relaxation time has the conventional value of 100 seconds (eq. 2) was used like a reference temperature instead of the calorimetric glass transition temperature, T_{gDSC}.

$$\log \tau = \log \tau_0 + B/(T - T_v) \quad (1)$$

$$T_{gDRS} = T_v + B/\log (100/\tau_0) \quad (2)$$

RESULTS

1. VFTH equation parameters and some characteristics defined with these parameters

The frequency dependence of dielectric losses "ε" for the α-relaxation at two temperatures, 400 and 420 K, is illustrated in Fig. 1. Here the lower temperature is located close to the glass transition domain, whilst the second temperature is well above this domain.

As expected, the α-peak shifts to higher frequencies (shorter relaxation times) as the temperature increases. It is observed that these peaks become extended as the temperature approaches glass transition temperature and the acceptor groups moiety is low (Fig. 1A), but the influence of polymer composition (w_A) on α-peak frequency (ω_α) is visible when the recording temperature is sufficiently high relative to T_{gDSC} (Fig. 1B).

Since T_{gDSC} values significantly strongly depend on the measurement parameters and taking into account that they do not characterize transitions between thermodynamic equilibrium states, the dielectric characteristics will be reported to the dielectric relaxation spectroscopy glass transition temperature, T_{gDRS} (eq. 7 – Experimental Section).

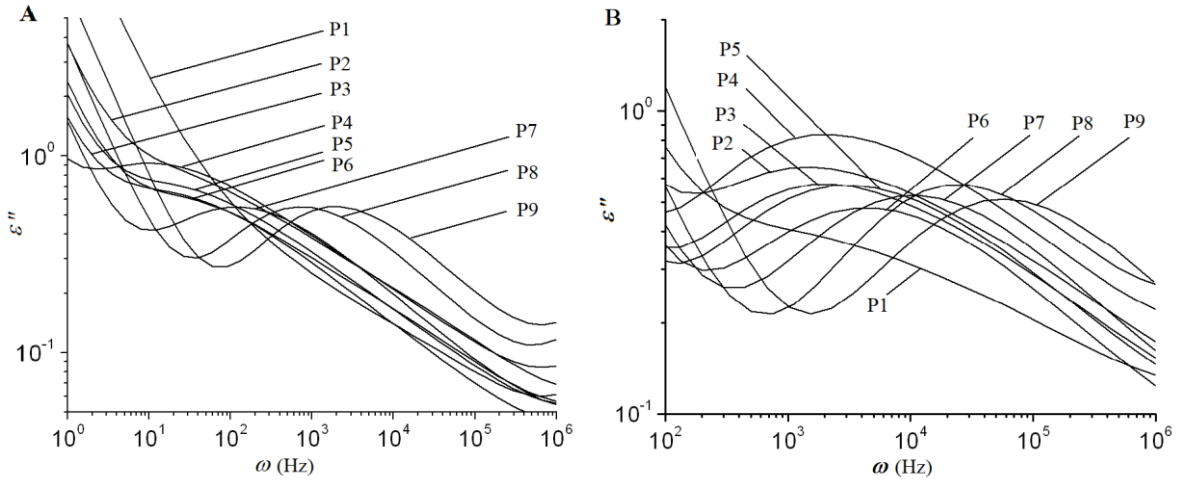

Fig. 1 – DRS spectra showing α-Relaxation peaks recorded at 400 K (127 ^{0}C) (A) and 420 K (147 ^{0}C) (B).

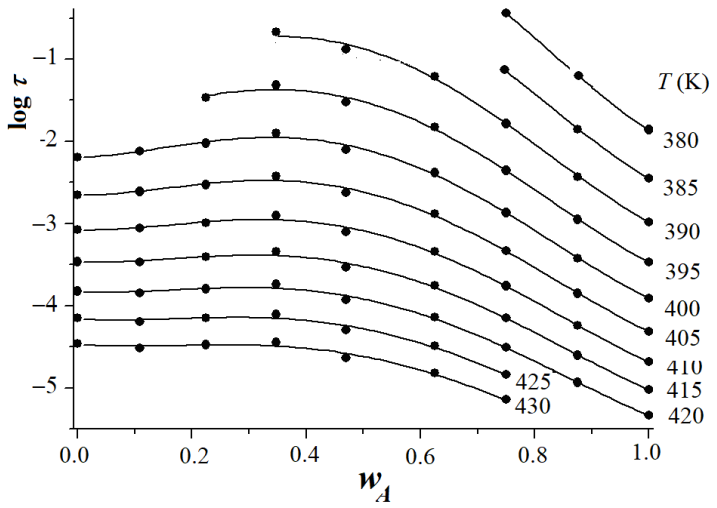

Fig. 2 – Plots logτ *versus* w_A for temperatures from 380 to 430 K and corresponding fitting curves.

The α-relaxation time values, obtained as previously presented, are plotted in Fig. 2 for each polymer at the temperatures used for recording the spectra. The τ values corresponding to too distorted

signals are omitted, but those corresponding to temperatures higher than 395 K were obtained without difficulty for the entire series of polymers. As can be seen, the isotherms show positive deviations from a monotonous decrease for the middle compositions, *i.e.*, where the density of donor-acceptor interactions is also maximum; the only explanation for this behavior is the slowing down of the molecular mobility caused by these interactions.

The values in Table 1 for the parameters T_v, $\log \tau_0$, and B were obtained by fitting $\log \tau$ dependences on $1/(T- T_v)$ as linear as possible by minimizing the deviation. This table contains also the values resulting for T_{gDRS} as well as for the free volume expansion coefficient, $a_f=1/B$, kinetic free volume fraction, $f_c=(T_{gDRS} - T_v)/B$[30] and fragility index, $m=m_0/(1-T_v/T_{gDRS})$ where $m_0 = \log \tau_g - \log \tau_0 = 2- \log \tau_0$ is the fragility for purely Arrhenius dynamics.[22] As observed, T_{gDRS} is lower than T_{gDSC} by 13 to 20 degrees for each polymer sample.

Table 1

The values found for the parameters of the VFTH equation and characteristics calculated with them.

Sample	w_A	T_v(K)	$\log \tau_0$	B (K)	T_{gDRS}(K)	$10^3 a_f$ (K^{-1})	$10^2 f_c$	m	T_v/ T_{gDSC}	T_{gDRS}/ T_{gDSC}
P1	0	274	–14.04	1448.4	364.3	0.690	6.24	66.14	0.73	0.96
P2	0.11	282	–13.74	1427.6	372.7	0.701	6.35	64.68	0.73	0.97
P3	0.22	298	–13.06	1138.5	373.6	0.878	6.64	74.42	0.77	0.96
P4	0.38	301	–12.71	1088.5	375.0	0.918	6.79	74.54	0.77	0.96
P5	0.47	306	–12.36	957.8	372.7	1.044	6.96	80.24	0.78	0.95
P6	0.62	292	–13.86	1251.3	370.9	0.799	6.30	74.55	0.75	0.95
P7	0.75	276	–14.58	1454.1	363.7	0.688	6.03	68.76	0.72	0.94
P8	0.87	255	–16.12	1846.4	356.9	0.541	5.52	63.46	0.67	0.94
P9	1	243	–17.32	2136.7	353.6	0.468	5.17	61.77	0.64	0.94
						Average values	**0.73**	**0.95**		

2. Electrical dc conductivity

The dc conductivity values obtained by the procedure presented before are plotted in Fig. 3. It is worth noting that (i) the plots for temperatures between 390 and 400 K seem to present relative maxima for w_A situated between 0.4 and 0.8 and (ii) the rate of variation with temperature differs from one polymer to another, increasing in the order P1<P5<P6<P3<P2<P7<P4<P8<P9. The values corresponding to the T_{gDRS} temperature are analyzed in the discussion section.

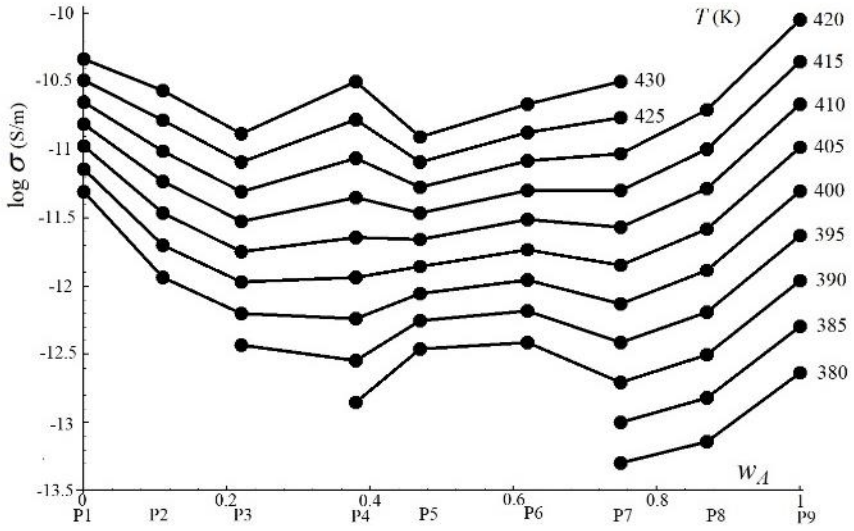

Fig. 3 – Discrete plots in logarithmic scale for the dc conductivity in S/m at different temperatures as resulted from spectra for each polymer composition by using HN equations.

DISCUSSION

1. Influences of D-A interactions on VFTH parameters

Figure 4 graphically illustrates the dependence of the parameters T_v, τ_0, B, T_{gDRS}, a_f, and m presented in Table 1 on the content of electron acceptor groups as well as on the ratio between the numbers of donor and acceptor groups. An interesting result is that these dependencies deviate significantly from monotony; maxima are located in the equimolar composition range (w_A = 0.5 ± 0.1), where the probability of donor-acceptor interactions is maximum. An exception is slope B in the VFTH equation, which shows negative deviation (considered normal) since this is the inverse of the characteristic a_f. The positive deviation is explained in the case of Vogel-Fulcher and glassy transition temperatures, T_v and T_{gDRS}, as well as for the dielectric relaxation time, τ_0, by the slowing down of molecular mobility due to the interactions between electron donor and acceptor groups, whose effect is somewhat similar to that of crosslinks.[17] This deviation is also explainable for the free volume expansion coefficient and kinetic free volume fraction, a_f, and f_c, both at T_{gDRS}, because the free volume, namely the volume that is not occupied by polymer chains themselves, is increased because the donor-acceptor interactions constrain the polymer chains.

Regarding to the fragility index, two aspects seem less understood: (1) the relatively small values (Table 1), which are comparable to those of low-molecular glass-forming liquids (m<100) and significantly lower than those of common polymers (100÷200)[22,30] as well as (2) the fact that the donor-acceptor interactions increase the fragility, that is, these interactions narrow the glass-transition temperature range. However, due to their large and deformed corresponding DSC signals, this second aspect could not be confirmed.

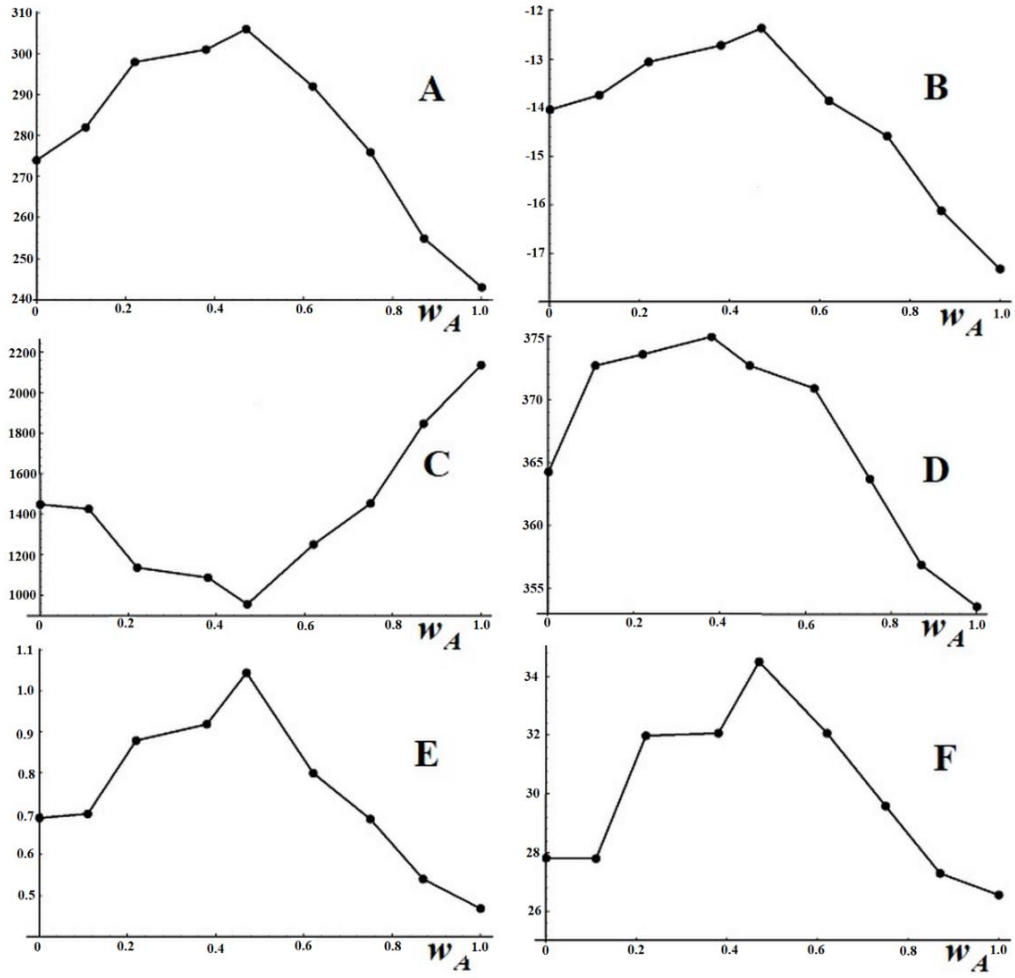

Fig. 4 – How the VFTH and derived parameters depend on the amount of acceptor groups: T_v (A), log τ_0 (B), factor B (C), T_{gDRS} (D), $10^3 a_f$ (E) and fragility index m (F).

Another observation concerns the values of the T_v/T_{gDSC} ratio, which are distributed between 0.64 and 0.78 (Table 1). An average ratio of 0.73 could be considered close to the value of 0.77 established by Bestul and Chang from calorimetric measurements[31] and Adam and Gibbs from viscometric data.[32] This is proven by Liu *et al.*[33] who generate quite linear VFTH diagrams for amorphous polymers even in the non-Arrhenius region Tg < T < 1.3 Tg. But our system deviates from this trend, this aspect could support the hypothesis that D-A interactions can strongly influence the glass transition.

2. About the dc electrical conduction

To further highlight how the dc electric conductivity depends on the copolymer composition, its values were calculated for the DRS glass transition temperature, T_{gDRS}, *i.e.*, in states with the same rate of segmental mobility. As the eq. 7 (Experimental section) does not apply in the range of glass transition temperatures, these values were calculated by using the empiric relationship 3, which is the logarithmic form of Mott's relationship, $\sigma = \sigma_0 \exp[-(T_0/T)^{1/4}]$,[34] whose parameters c and d (Table 2) were established by fitting the values plotted in Fig. 3.

$$\log \sigma(T) = c + d\, T^{-1/4} \qquad (3)$$

It can be seen from Fig. 5 that the dependence of conductivity on polymer composition deviates from monotony with a maximum in the equimolar composition region, which suggests that the total conductivity, σ_t, has two components, a component σ_i, that decreases monotonously with w_A, and the other, σ_e, with a maximum at about $w_A = 0.5$. As is known, the electric charge carriers in dielectric/insulating polymers, as in our study, can be positive and negative ions, in the case of ionic conduction[35] and electrons and holes, in the case of hopping conduction.[36] Ions are formed by the chemical impurities ionization and/or due to molecular structure imperfections through the applied electric field. The generation of electron-hole pairs occurs due to the jump of electrons from donor groups to acceptor groups, favored by charge-transfer interactions between these groups. In our case, the σ_i component would be ionic-type conductivity associated with structural defects of the sequences of electron donor units whose concentration would normally decrease with w_A, while the σ_e component would be electronic conductivity that increases normally with the density of donor-acceptor interactions whose maximum occurs at $w_A = 0.5$. In support of the assumption of electronic conduction is the fact that the donor-acceptor copolymers show photoconduction, which is par excellence hopping conduction through electron-hole pairs with a maximum at $w_A = 0.5$.[12–14]

Table 2

The parameters c and d of relationship 3 and dc conductivity values at T_{gDRS} for each polymer composition.

Sample	w_A	c	d	log $\sigma(T_{gDRS})$
P1	0.00	43.13	–243.46	–12.40
P2	0.11	64.53	–341.96	–13.31
P3	0.22	61.37	–329.01	–13.59
P4	0.38	84.76	–433.79	–13.70
P5	0.47	52.08	–286.81	–13.10
P6	0.62	60.11	–322.29	–13.34
P7	0.75	78.61	–405.97	–14.20
P8	0.87	85.38	–434.98	–14.38
P9	1.00	92.13	–462.56	–14.50

Mathematically, the σ_i curve in the figure was obtained assuming that (i) the electronic conduction is absent when w_A is equal to 0 and 1, and negligible when w_A is equal to 0.13 and 0.87, that is when the density of D-A interactions is null or negligible (samples P1, P2, P8 and P9), and (ii) supposing that the fitting function is a polynomial function of the third degree. The electronic conductivity was obtained as the difference from relationship (4). The values of the three types of conductivities at T_{gDRS} are given for each polymer composition in Table 3. It is understood that the values for σ_i and σ_e depend to some extent on the assumed dependence $\sigma_i(w_A)$, but this does not cancel the presence of two electrical conductions.

$$\sigma_e = \sigma_t - \sigma_i = 10^{\log \sigma t} - 10^{\log \sigma i} \qquad (4)$$

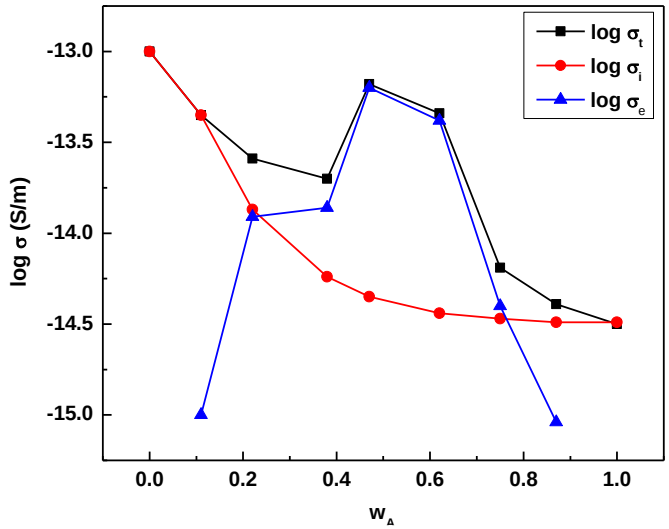

Fig. 5 – Logarithmic values of dc conductivities in S/m at T_{gDRS} plotted *versus* polymer composition: the total conductivity σ_t and its decomposition in ionic and electronic components, σ_i and σ_e.

Table 3

The components of dc conductivities at T_{gDRS} for different polymer compositions.

w_A	0	0.11	0.22	0.38	0.47	0.62	0.75	0.87	1
10^{13} σ_t (S/m)	3.981	0.446	0.256	0.196	0.663	0.452	0.064	0.041	0.032
10^{13} σ_i (S/m)	3.981	0.446	0.134	0.057	0.045	0.036	0.034	0.032	0.032
10^{13} σ_e (S/m)	0	<0.001	0.122	0.139	0.618	0.416	0.039	<0.009	0

The phenomenon of coupling between the segmental α-relaxation and the conductivity is often discussed concerning the Stokes-Einstein (eq. 5):[37]

$$\sigma\, T\, \tau \sim \tau^{e} \qquad (5)$$

where σ, τ, and T are dc conductivity, polymer segmental relaxation time and temperature, respectively. This relationship applies to ionic conduction in coupled systems at $T=T_{gDRS}$, and the exponent e equals zero. In this work, we find that the exponent e has values between 0.29 and 0.66, the lowest values being characteristic for the samples with $w_A > 0.75$, *i.e.*, when the electronic conduction is negligible. Therefore, we consider that the coupling in question is insignificant in our polymers, and this is further evidence of the electronic conduction.

EXPERIMENTAL

1. Polymers: Synthesis and Relevant Characteristics

The polymers were obtained by radical polymerization and purified by precipitation in methanol from THF solutions.[23] Reaction media whose fraction of acceptor comonomer, W_A, was 0.0, 0.125, 0.25, 0.375, 0.50, 0.625, 0.75, 0.875, and 1.0 were used, resulting in polymers with the fractions of acceptor units, w_A, from Table 4. The polymer samples are marked from P1 to P9, starting with $w_A = 0$.

Molecular characteristics, such as w_A composition, were determined from 1HNMR spectra using a Bruker Avance DRX 400 MHz ^{1}HNMR spectrometer (at room temperature and CDCl3 solutions). The average molecular weight, Mw, was found from triplicates of MALS measurements performed in THF using a Wyatt DAWN DSP MALS photometer (equipped with a 633 nm HeNe laser) and supplemented with a Wyatt Optillab rEX differential refractometer. Glass transition temperatures were determined with a DSC instrument (Perkin Elmer Pyris, USA), after a second heating scan at 10 K/min, samples of approximately 8–9 mg were heated in N2 flow (20 ml/min). All experimental results are presented in Table 4.

The sequence distribution of the copolymers was random because their compositions were equal to those of the corresponding reaction media within the limits of experimental error, which has been a well-known synthesis-structure correlation for many years.[24] In addition, the investigated polymers are predominantly syndiotactic because the splitting

of the methyl proton NMR signals showed that the probability of (co)syndiotacticity is 0.75÷0.77. Such chain microstructure characteristics would explain that the sample fracture reliefs observed by AFM are rather smooth, without voids and sharp profiles.

As shown in Table 4, the molecular mass decreases with the fraction of EA units, exhibiting a wide minimum for samples P6 and P7. However, the lowest values of Mw must be larger than 30 kDa, which is considered the lowest value from which the glass transition temperature no longer depends on the polymer weight.[25]

The DSC glass transition temperature, T_{gDSC}, shows a weak maximum placed at w_A = 0.4÷0.5. Relative to the average value of the two homopolymers, here the maximum increases by about 3% in Kelvin degrees and 12% in Celsius degrees. A relatively weak dependence of T_{gDSC} *vs* composition indicates that the weak D-A complexation interactions characterize the copolymers studied. Such dependence could be explained using the Fox-Loshaek equation[17] where the crosslink density would be replaced with that of D-A associations. In addition, the proton NMR spectra confirmed that the complexes in solution are of 1:1 type, with a parallel π-donor-π-acceptor planar arrangement.[26] Other characteristics besides those in Table 4 can be found elsewhere.[23]

Table 4

Data about the composition, molecular weight, and DSC glass transition temperature of the studied polymers.
W_A is the molar fraction of EA monomer at feeding.

Sample	W_A	w_A	dn/dc (mL/g)	M_w (kDa)	T_{gDSC} (K)
P1	0.0	0.0	0.210	120.0	380.4
P2	0.125	0.11	0.198	100.7	385.4
P3	0.25	0.22	0.187	81.4	388.2
P4	0.375	0.38	0.175	67.4	391.3
P5	0.5	0.47	0.165	54.5	391.4
P6	0.625	0.62	0.159	48.1	388.6
P7	0.75	0.75	0.155	43.1	385.6
P8	0.875	0.87	0.141	62.4	380.4
P9	1.0	1.0	0.126	83.4	377.1

2. Measurements

Samples for measurements were prepared directly between two round metallic plates, thus forming a capacitor that was used in all the measurements. First, a pellet of 13 mm diameter and 0.6–0.7 mm thickness obtained from 100 mg polymer powder by compressing at room temperature was introduced between two stainless steel discs of 20 mm diameter and lightly pressed under nitrogen into the dielectric spectrometer measuring cell during heating from room temperature up to 170 °C with a rate of 10 °C/min. After a stationary time of 5 minutes at 170 °C, the cell temperature was decreased by 10 ^{0}C/min until –100 ^{0}C, *i.e.*, until the starting temperature of the dielectric measurements. The elastic tension that usually ensures electrode-sample-electrode contact in the measuring cell was the compressing force of the spring. This force spreads the molten polymer over the entire surface of the electrodes if applied in a temperature range above Tg but below 200 °C, where thermal degradation is possible to start. The excess polymer was removed. As spacers, three small strips of 0.125 mm thick Kapton film (DuPont) were placed on the edge of the electrode. It is relevant that the total area of the spacers was only 4–6% of the electrode surface, and the Kapton film used shows only a weak relaxation at 400 K, which does not affect the much stronger relaxation signals of the studied polymers. Finally, for each polymer in the series, flat capacitor samples were obtained containing pairs of metal disk electrodes separated by 0.125 mm thick polymer layers. The thickness of the polymer layer may differ slightly between samples, but this does not affect the temperature and frequency dependences of the permittivity, and possible small deviations of the absolute values of the permittivities ε' and ε" are not discussed in this article.

The measurements were performed without removing the sample from the measuring cell. Isothermal spectra were recorded between 100–106 Hz, while temperatures from 380 to 430 K were changed in 5 K steps. A Concept 40 dielectric spectrometer was equipped with a Quatro thermostat and a ZGS measuring cell from Novocontrol was used. The operational control and primary data processing were performed using the WinDeta-WinFit software based on the HN approach, also from Novocontrol. This program allowed the determination of the α-relaxation times from the corresponding ε" spectra in the frequency domain by fitting them to the HN equation 6, whose right-hand side contains terms for α-relaxation[27] and conductivity effects resulting from the theory of electrical relaxation of materials.[28,29] The HN function contains: (i) the relaxed ($\omega \rightarrow 0$) and un-

relaxed ($\omega\rightarrow\infty$) values of the dielectric constant, ε_r and ε_u, respectively, (ii) the HN relaxation time for the considered process, τ_{HN}, and (iii) a and b exponential factors which represent the broadening and skewing parameters, respectively. Other parameters in eq. 3 are the dc conductivity corresponding to zero frequency of the electric field, σ, an exponential factor, n, the permittivity of free space, ε_0, and the frequency of the applied field, ω. For a given temperature, the relaxation time, τ, associated with the position of the relaxation peak is derived from the corresponding HN relaxation time according to eq. 7.

$$\varepsilon(\omega) = \{\varepsilon_u + (\varepsilon_r - \varepsilon_u)/[1 + (i\omega\tau_{HN})^a]^b\} - i(\sigma/\varepsilon_0\omega)^n \quad (6)$$

$$\tau = \tau_{HN}\{\sin[\pi ab/(2 + 2b)]/\sin[\pi a/(2 + 2b)]\}^{1/a} \quad (7)$$

The aforementioned Novocontrol software provided values for the corresponding dielectric parameters as well as for the conductivity of the samples at each temperature used for recording the spectra.

CONCLUSIONS

We found that HN analysis of dielectric spectra recorded by frequency scanning at different temperatures shows that D-A interactions impose a slowdown of segmental mobility, proved by an increase in the VFTH equation parameters (T_v and log τ_0) and their associated characteristics T_{gDSC}, a_0, f_0 and m, their maxima being associated with the maximum D-A interactions.

Another conclusion of this study is that such spectra in these types of polymers can reveal that the electrical conduction, summing the ionic conduction, is due to the ionization of ED groups. Moreover, the electronic conduction occurs in jumps due to charge transfer between DA and EA groups.

Acknowledgment. The authors are grateful to Dr. M. Grigoras from "Petru Poni" Institute of Macromolecular Chemistry of Iasi for the kind supply of the polymer samples.

REFERENCES

1. M. Scarongella, A. Laktionov, U. Rothlisberger and N. Banerji, *J. Mat. Chem. C*, **2013**, *1*, 2308–2319.
2. J. M. Pearson, "Photoconductive polymers", in "Photochemical Processes in Polymer Chemistry-2", G. Smets – Pergamon Press (Ed.), **1977**, pp. 463–477.
3. J. Thomas, C. W. Christenson, P. A. Blanche, M. Yamamoto, R. A. Norwood and N. Peyghambarian, *Chem. Mat.*, **2011**, *23*, 416–429.
4. N. Zhou, A. S. Dudnik, T. I. N. G. Li, E. F. Manley, T. J. Aldrich, P. Guo, H.-C. Liao, Z. Chen, L. X. Chen, R. P. H. Chang, A. Facchetti, M. Olvera de la Cruz and T. J. Marks, *J. Am. Chem. Soc.*, **2016**, *138*, 1240–1251.
5. S. Karuthedath, J. Gorenflot, Y. Firdaus, Y. Firdaus, N. Chaturvedi, C. S. P. De Castro, G. T. Harrison, J. I. Khan, A. Markina, A. H. Balawi, T. A. Dela Peña, W. Liu, R. Z. Liang, A. Sharma, S. H. K. Paleti, W. Zhang, Y. Lin, E. Alarousu, S. Lopatin, D. H. Anjum, P. M. Beaujuge, S. De Wolf, I. McCulloch, T. D. Anthopoulos, D. Baran, F. Laquai, *Nat. Mater.*, **2021**, *20*, 378–384 https://doi.org/10.1038/s41563-020-00835-x
6. X. Ma, Q. Fu, J. Chen, X. Chen, H. Gao and A. K. Y. Jen, *Science China Materials*, **2024**, https://doi.org/10.1007/s40843-024-3191-4.
7. C. I. Simionescu, V. Percec and A. Natansohn, *Polymer*, **1980**, *21*, 417–422.
8. C. I. Simionescu, V. Barboiu and M. Grigoras, *J.Macro. Sci.: Part A-Chem*, **1985**, *22*, 693–711.
9. M. Grigoras, "Conductive polymers: From synthesis to properties and applications", Memoirs of the Scientific Sections of the Roumanian Academy, Tome XLIII, **2020**, 29–45.
10. U. Epple and H. A. Schneider, *Thermochim. Acta*, **1990**, *160*, 103–112.
11. A. Simmons and A. Natansohn, *Macromol.*, **1991**, *24*, 3651–3661.
12. C. I. Simionescu, M. Grigoras and V. Barboiu, *Pol. Bull*., **1983**, *9*, 577–581.
13. C. I. Simionescu, V. Barboiu and M. Grigoras, *Pol. Bull*., **1984**, *11*, 545–550.
14. A. Natansohn, *J. Pol. Sci: Pol. Chem. Ed*., **1984**, *22*, 3161–3171.
15. M. J. Schroeder, C. M. Roland and T. K. Kwei, *Macromol*., **1999**, *32*, 6249–6253.
16. D. E. Buerger and R. H. Boyd, *Macromol.*, **1989**, *22*, 2694–2699.
17. J. K. W. Glatz-Reichenbach, L. Sorriero and J. J. Fitzgerald, *Macromol*., **1994**, *27*, 1338–1343.
18. C. V. Grigoras and A. G. Grigoras, *J. Therm. Anal. Calorim.*, **2011**, *103*, 661–668.
19. H. Vogel, *Phys. Z.*, **1921**, *22*, 645–646.
20. G. S. Fulcher, *J. Am. Cer. Soc*., **1925**, *8*, 339–355.
21. G. Tammann and W. Hesse, *Zeitschrift für anorganische und allgemeine Chemie*, **1926**, *156*, 245–257.
22. V. N. Novikov and A. P. Sokolov, *Entropy*, **2022**, *24*, 1101, https://doi.org/10.3390/e24081101.
23. C. I. Simionescu, E. Bicu, M. Grigoras and V. Barboiu, *Eur. Pol. J.*, **1984**, *20*, 1053–1056.
24. F. R. Mayo and C. Walling, *Chem. Rev.*, **1950**, *46*, 2, 191–287, https://doi.org/10.1021/cr60144a001 .
25. T. B. Blythe, "Electrical properties of polymers", 2 edition, Cambridge University Press, Cambridge, 2005.
26. V. Barboiu, A. G. Grigoras, V. C. Grigoras and G. L. Ailiesei, *Rev. Roum. Chim*, **2012**, *57*, 151–157.
27. S. Havriliak and S. Negami, A, *Polymer*, **1967**, *8*, 161–210.
28. G. T. Williams and D. K., Novocontrol Applications Note, *Dielectrics*, **1998**, *3*, 23–25.

29. A. K. Schonhals, “Broadband Dielectric Spectroscopy”, Springer Verlag, Berlin Ed., 2003.
30. R. Böhmer, K. L. Ngai, C. A. Angell and D. J. Plazek, *J. Chem. Phys.*, **1993**, *99*, 4201–4209.
31. A. B. Bestul and S. S. Chang, *J. Chem. Phys.*, **1964**, *40*, 3731–3733.
32. G. Adam and J. H. Gibbs, *J. Chem. Phys*., **1965**, *43*, 139–146.
33. C. Y. Liu, J. He, R. Keunings and C. Bailly, *Macromol.*, **2006**, *39*, 8867–8869.
34. N. F. Mott, *The Phil. Mag.: J. Theor.Ex. and Appl.Phys.*, **1969**, *19*, 835–852.
35. T. Miyamoto and K. Shibayama, *J. Appl. Phys.*, **1973**, *44*, 5372-5376.
36. V. F. Gantmakher, "Hopping conductivity", Chapter 4, “Electrons and Disorder in Solids”, Oxford Academic (Ed.), 2005, pp. 58–73, doi.org/10.1093/acprof:oso/9780198567561.003.0004
37. T. Dam, S. S. Jena and D. K. Pradhan, *Phys. Chem. Chem. Phys.*, **2016**, *18*, 19955–19965.